AGU PUBLICATIONS

Water Resources Research

RESEARCH ARTICLE
10.1002/2016WR019104

Key Points:
- Tap water isotopes reflect urban water system structure and management practices
- Isotopic patterns linked to political boundaries and demographic factors across Salt Lake Valley
- Evaporation from city water sources increased by >9400 m^3/day during unusually warm, dry years

Supporting Information:
- Supporting Information S1

Correspondence to:
Y. Jameel,
yusuf.jameel@utah.edu

Citation:
Jameel, Y., S. Brewer, S. P. Good, B. J. Tipple, J. R. Ehleringer, and G. J. Bowen (2016), Tap water isotope ratios reflect urban water system structure and dynamics across a semiarid metropolitan area, *Water Resour. Res.*, *52*, doi:10.1002/2016WR019104.

Received 20 APR 2016
Accepted 7 JUL 2016
Accepted article online 14 JUL 2016

Tap water isotope ratios reflect urban water system structure and dynamics across a semiarid metropolitan area

Yusuf Jameel[1], Simon Brewer[2], Stephen P. Good[3], Brett J. Tipple[4,5], James R. Ehleringer[4,5], and Gabriel J. Bowen[1]

[1]Department of Geology and Geophysics, University of Utah, Salt Lake City, Utah, USA, [2]Department of Geography, University of Utah, Salt Lake City, Utah, USA, [3]Department of Biological and Ecological Engineering, Oregon State University, Corvallis, Oregon, USA, [4]Department of Biology, University of Utah, Salt Lake City, Utah, USA, [5]IsoForensics Inc., Salt Lake City, Utah, USA

Abstract Water extraction for anthropogenic use has become a major flux in the hydrological cycle. With increasing demand for water and challenges supplying it in the face of climate change, there is a pressing need to better understand connections between human populations, climate, water extraction, water use, and its impacts. To understand these connections, we collected and analyzed stable isotopic ratios of more than 800 urban tap water samples in a series of semiannual water surveys (spring and fall, 2013–2015) across the Salt Lake Valley (SLV) of northern Utah. Consistent with previous work, we found that mean tap water had a lower ^{2}H and ^{18}O concentration than local precipitation, highlighting the importance of nearby montane winter precipitation as source water for the region. However, we observed strong and structured spatiotemporal variation in tap water isotopic compositions across the region which we attribute to complex distribution systems, varying water management practices and multiple sources used across the valley. Water from different sources was not used uniformly throughout the area and we identified significant correlation between water source and demographic parameters including population and income. Isotopic mass balance indicated significant interannual and intra-annual variability in water losses within the distribution network due to evaporation from surface water resources supplying the SLV. Our results demonstrate the effectiveness of isotopes as an indicator of water management strategies and climate impacts within regional urban water systems, with potential utility for monitoring, regulation, forensic, and a range of water resource research.

1. Introduction

Supplying water to urban areas within water-limited regions requires accessing, managing, and allocating water from an intricate network of sources to provide safe, drinkable water at the point of use. Expanding population and agricultural production has increased the vulnerability of water supplies and made availability of sustainable water resources to urban areas a major challenge. In order to successfully meet rising demands, water managers have resorted to overexploitation of regional surface water resources, large-scale interbasin transfer, and extraction from subsurface aquifers [*Rodell et al*., 2009; *Fort et al*., 2012]. These processes have significantly altered regional ecohydrological systems especially in arid and semiarid regions where water is scarce [*Seckler et al*., 1999; *Bates et al*., 2008; *Buckley*, 2013]. Further, significant changes in the spatial and temporal distribution of water within urban areas (relative to the natural, undeveloped landscape) modify the energy balance, ecohydrology, and biogeochemical processes of cities [*Chen et al*., 2006; *Kuttler et al*., 2007]. Thus, there is an increasing need to understand the connections among human populations, climate, water extraction, water supply, and water use impacts in semiarid regions undergoing rapid urbanization.

Stable isotopes of H and O in water are geochemical tracers that vary systematically in their natural abundance throughout the global hydrological cycle, and thus, preserve information on the climatological source of the water and its postprecipitation history. Precipitation events preferentially distill heavy isotopes from the atmosphere, resulting in variation in isotopic ratios of precipitation along gradients of continentality, latitude, altitude, and temperature [*Craig*, 1961; *Dansgaard*, 1964; *Bowen and Wilkinson*, 2002]. Environmental waters, such as ground and surface water, are derived from meteoric precipitation and in the most cases

have isotopic ratios similar to the regional precipitation [*Gat*, 1996; *Smith et al*., 2002; *Bowen et al*., 2012]. Within terrestrial hydrological systems, stable H and O isotope ratios are largely conservative tracers, the major exception being the strong effect of evaporation, which produces vapor depleted in ^{2}H and ^{18}O and thus leads to an increase in the isotopic ratios of the residual water. Given the significant amount of provenance information recorded in the stable isotopes of water, they have been widely applied in various climatological, ecological, and hydrological studies [*Grootes et al*., 1993; *Hobson et al*., 1999; *Darling*, 2004; *Aggarwal et al*., 2005; *Fry*, 2007]. Recent studies have shown that isotope ratios of waters within human-managed hydrological systems also incorporate distinctive information on the geographical origin of waters and hydrological processes within these systems [*Bowen et al*., 2005b; *O'Brien and Wooller*, 2007; *Ehleringer et al*., 2008; *Dawson and Siegwolf*, 2011; *Good et al*., 2014a; *Landwehr et al*., 2014]. These studies have investigated tap water isotope patterns across large (regional to country-level) spatial scales [*Bowen et al*., 2007b; *Landwehr et al*., 2014]; however, few studies have documented tap water isotope patterns at scales where the effects related to the physical (pipelines) and political (water management units) infrastructure of cities might be clearly expressed [*Leslie et al*., 2014; *Ehleringer et al*., 2016].

Water managers have traditionally used pipe network analyses to predict the flow rates and calculate head losses in urban water supply networks. These analyses are based on conservation of mass and energy and use iterative algorithms to predict the flow within the system [*Gupta and Bhave*, 1994]. Even though the estimation of flow rates, pressure gradients, and head losses by these techniques are generally robust, they are computationally intensive and suffer from several shortcomings, such as absence of a unique solution for an underdetermined system, assumption of invariant flow rates, and noninclusiveness of uncertainty in the analysis [*Waldrip et al*., 2016]. These calculations also require detailed information such as node elevation, pipe diameter, length, roughness, and pump operating data among many other variables to track the flow. In many cities, results obtained from these techniques can be prone to error due to outdated/incorrect information on the water supply infrastructure [*Liggett and Chen*, 1994]. Further, the accuracy of the results obtained from these models is difficult to verify (M. Owens and J. Hilbert, personal communications with SLC water managers, 2015). In other cases, water supply infrastructure information may be considered proprietary, or difficult to obtain due to security concerns, or may be lacking in cities in underdeveloped and developing countries. In such cases, water isotopes provide a promising observational technique to evaluate the function of water distribution systems and establish connections between water in these systems and environmental sources. Combining high-resolution spatiotemporal isotope data from within the supply system with basic water infrastructure information and volumetric data may provide a basis for estimation of flow pattern within the supply system.

Here we present results from an urban-scale spatiotemporal tap water survey of stable isotopes, conducted in the Salt Lake Valley metropolitan area (SLV) of northern Utah, USA. We analyzed ^{2}H and ^{18}O data in the Salt Lake Valley (SLV) in the context of known water management boundaries, water use, and climatic trends across a 3 year study period. We observed coherent spatiotemporal pattern within SLV comprising of distinct isotopic regions that reflect both commonalities and differences in the water management practices and multiple source water among the water districts of the SLV. We highlight the sensitivity of tap water isotopes to climatic change and the ability to identify potential links between demographic, socioeconomic factors, and water management practices using these tracers. Finally, we present our data as a predictive map of the tap water isotope ratios of the SLV, highlighting the temporally stable, spatially structured pattern of isotope ratios across the SLV. This "isoscape" could serve as a template for understanding the propagation of SLV municipal water throughout the hydrological cycle (infiltration to groundwater, evapotranspiration etc.), forensic, and ecological studies where understanding of local-scale variations and patterns are extremely important [*Darling et al*., 2003; *Bowen et al*., 2005a; *Kennedy et al*., 2011], and monitoring and enforcement of water rights in a system consisting of a complex array of public and private stake holders.

2. Methods

2.1. Site Description

The SLV lies within the Great Salt Lake Basin, a closed semiarid basin in western North America that encompasses parts of Utah, Nevada, Wyoming, and Idaho. The current population of the SLV is more than 1

Table 1. Annual Average Temperature, Annual Total Precipitation, and Their Deviation From the Long-Term Average Measured at the Salt Lake City International Airport (SLC)[a]

Year	Average Temperature (°C)	Deviation (°C)	Average Precipitation (mm)	Deviation (mm)
2010	10.8	−0.3	347	−72
2011	11.2	0.1	600	181
2012	13.1	2.0	288	−131
2013	12.4	1.3	335	−84
2014	12.4	1.3	393	−26
2015	13.7	2.6	360	−59

[a]The annual values are calculated for the individual water year (1 October of the previous year to 30 September of the current year). The normal annual average temperature and total precipitation (measured from 1971 to 2000) are 11.1°C and 419 mm for SLC. (Source: NOAA climate data, http://www.ncdc.noaa.gov/IPS/cd/cd.html).

million, and is expected to almost double by 2060 (http://governor.utah.gov/DEA/demographics.html). The SLV is surrounded by the Great Salt Lake towards the north, the Wasatch, Oquirrh, and Traverse Mountains on the east, west and south, respectively, and is relatively dry with annual average precipitation less than 500 mm. In contrast, the adjoining mountains receive significantly higher amounts of precipitation, in excess of 1250 mm at the higher elevations [*Baskin et al.*, 2002]. The climate of the SLV is highly seasonal, with dry, warm summers and cold, wet winters. Average valley temperatures and yearly precipitation amounts during the 3 year study period were approximately 12.8°C and 362 mm, respectively, which were considerably higher and lower, respectively, than long-term averages (Table 1).

The urban portions of the SLV are divided into 18 water management districts (hereafter "districts"; Figure 1), most of which oversee service areas that correspond with municipal political boundaries. These districts serve as water brokers for their ratepayers, in some cases producing water from locally managed sources, but more commonly districts purchase and distribute water from regional wholesalers. Districts within SLV provide municipal water sourced from several creeks from the Wasatch Mountains (hereafter, Wasatch Creeks), the Provo River-Jordanelle Reservoir-Deer Creek Reservoir system (subsequently referred to as Provo River System) from the Uinta Mountains (∼20 km east of the SLV), and numerous groundwater wells situated throughout valley. Two wholesalers manage the major surface water projects, with the Provo River System operated primarily by the Jordan Valley Water Conservation District (JVWCD) and the Wasatch Creeks overseen by the Metropolitan Water District of Salt Lake and Sandy (MWD). Both the JVWCD and MWD also extract groundwater from wells within the SLV. Most SLV water districts purchase some or all of their water from the JVWCD or MWD (Figure 1), while a small number of districts provide all or most of their culinary water from wells within the district or supplement purchased water with water extracted from local wells.

2.2. Sample Acquisition

Samples were collected semiannually from 2013 to 2015, during the months of April (spring season) and September/October (fall season). In all, 816 samples were collected across all 18 districts. The total number of collection sites sampled during each survey varied between 116 (spring 2013) and 149 (fall 2013). This difference reflects the fact that some sites were sporadically sampled (subsequently referred to as intermittent sites), whereas 83 sites were sampled during all 6 surveys (as fixed sites; Figure 1). The latter are evenly distributed throughout the SLV, where the number of fixed sites per district relates to district size. Fixed sites per district ranged from 1 to 24 sites. Only one district (South Salt Lake City) did not include any fixed sites. Most statistical calculations presented here are based only on data from fixed sites.

Most samples were collected from taps in businesses and public facilities, with a small subset coming from private homes supplied by the local water district. Samples for each survey were collected on a single day, except for fall 2013 when five samples were collected 1 week after the main effort. For each site, samples were obtained by running the tap water for ∼15 s before filling, capping, and sealing (with Parafilm®) a clean 4 mL glass vial. The taps sampled in this study were regularly and frequently operated and we assumed insignificant fractionation occurring within the pipeline. SLV precipitation samples were collected throughout the study period using a custom-made funnel and bottle collector installed on the roof of the Frederick Albert Sutton Building, on the University of Utah campus. Thermostated heat tape placed within the collector was used to melt solid accumulation during cool-season precipitation events. Rainfall samples were collected daily after each significant precipitation event.

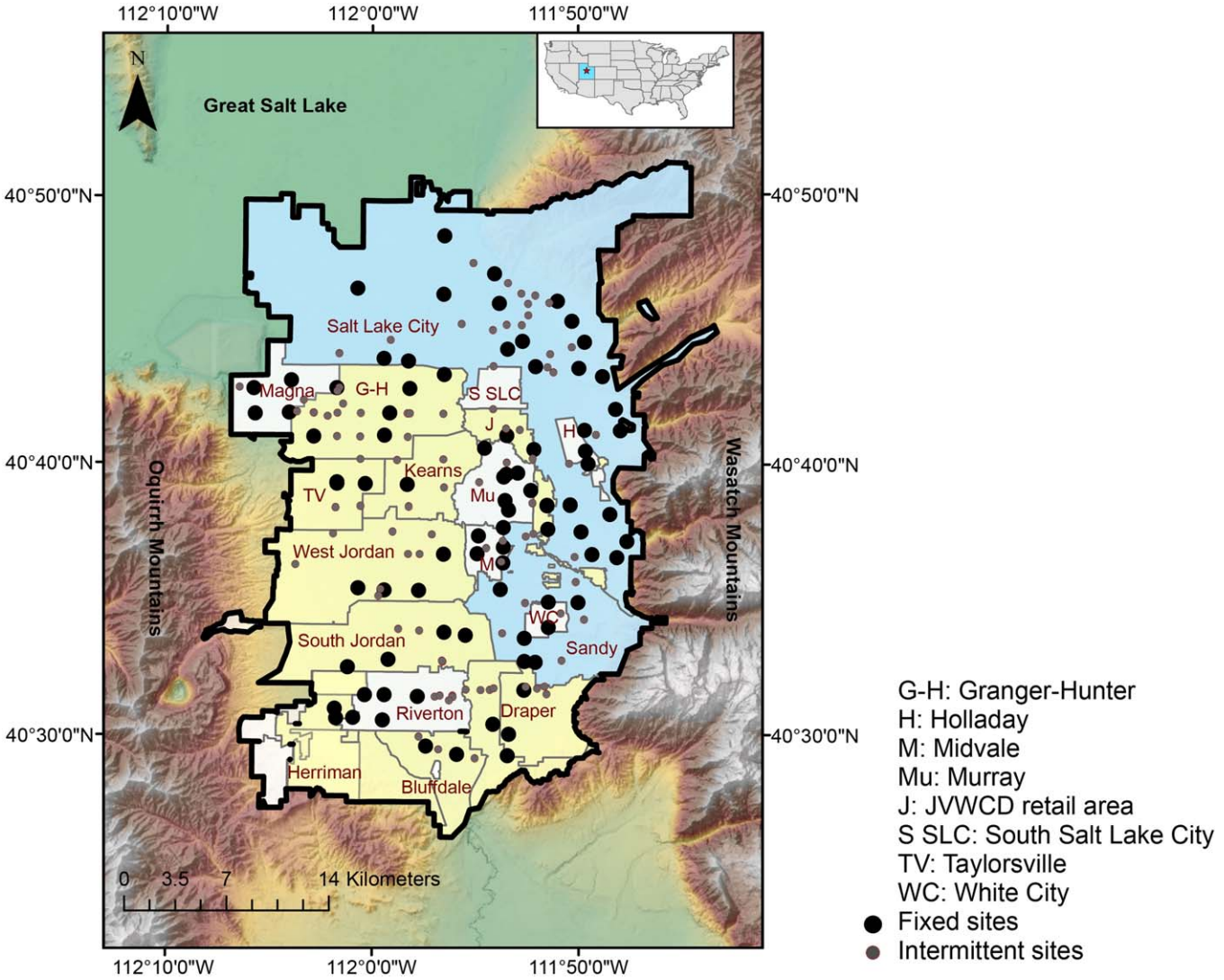

Figure 1. Tap water sampling sites within the 18 water districts of the SLV metropolitan area. The blue and yellow regions show areas serviced by MWD and JVWCD, respectively, throughout the study period; since 2015 the Riverton water district has been serviced by JVWCD.

The semiannual survey, in hydrologically contrasting seasons, was designed to capture potential seasonal differences in the tap water isotopes. As the largest isotopic differences in environmental water in the SLV have been previously observed during the spring and fall seasons [*Bowen et al*., 2007a], we opted for those periods. A similar strategy has previously been used in studying tap water isotope ratios across the United States, where sampling efforts were conducted in the months of February and August to capture seasonal differences in tap water isotopes [*Landwehr et al*., 2014].

2.3. Isotope Analysis

Prior to analysis, the samples were stored at 4°C in a refrigerator. The isotope ratios of samples were analyzed within a few weeks of their collection at the Stable Isotope Ratios for Environmental Research (SIRFER) facility, University of Utah, on a Cavity Ring-Down Spectroscopy (CRDS; Picarro L2130-i, Santa Clara, CA) analyzer. All the sample values are reported using δ notation, where $\delta = R_{sample}/R_{standard} - 1$, $R = {}^{2}H/{}^{1}H$ or ${}^{18}O/{}^{16}O$, and the VSMOW water standard is referenced. Four injections of each sample were measured and corrected for memory effects and through-run drift, and calibrated to the VSMOW-SLAP scale, using a suite of three laboratory reference waters (PZ: 16.9‰, 1.65‰; PT: −45.6‰, −7.23‰; UT: −123.1‰, −16.52‰; for δ^{2}H and δ^{18}O, respectively). Details of the calibration and correction procedure are reported in *Geldern and*

Table 2. Summary Statistics for the Stable Oxygen and Hydrogen Isotopic Composition and Deuterium Excess (*d*) for Samples Collected in the Salt Lake City Metropolitan Area From Spring 2013 to Fall 2015[a]

		All Sites				Fixed Sites			
Season		n	$\delta^{18}O$	$\delta^{2}H$	*d*	n	$\delta^{18}O$	$\delta^{2}H$	*d*
	Average		−15.9	−119.9	7.1		−15.9	−119.8	7.0
	SD		1.1	5.7	3.2		1.1	6.0	3.4
Spring 2013	Minimum	116	−17.5	−131.9	−6.0	83	−17.5	−131.9	−6.0
	Maximum		−11.5	−97.2	11.2		−11.5	−97.2	11.2
	Range		6.0	34.7	17.2		6.0	34.7	17.2
	Average		−15.6	−119.4	5.6		−15.6	−119.2	5.6
	SD		1.0	5.6	3.0		1.2	6.4	3.5
Fall 2013	Minimum	149	−17.2	−128.4	−5.5	83	−16.9	−125.3	−5.5
	Maximum		−11.1	−94.3	10.1		−11.1	−94.3	10.1
	Range		6.1	34.1	15.6		5.8	31.0	15.6
	Average		−15.8	−119.1	6.9		−15.7	−118.5	6.9
	SD		1.0	5.5	3.1		1.2	6.4	3.6
Spring 2014	Minimum	143	−17.0	−126.9	−5.5	83	−16.7	−122.8	−5.5
	Maximum		−11.1	−93.6	11.5		−11.1	−93.6	11.5
	Range		6.0	33.4	16.9		5.7	29.3	16.9
	Average		−15.6	−118.7	6.0		−15.5	−118.4	6.0
	SD		1.0	5.2	3.0		1.2	6.1	3.4
Fall 2014	Minimum	123	−17.0	−127.7	−5.5	83	−17.0	−125.4	−5.5
	Maximum		−11.3	−96.0	10.9		−11.3	−96.0	10.9
	Range		5.7	31.7	16.4		5.7	29.4	16.4
	Average		−15.6	−117.9	6.5		−15.5	−117.6	6.5
	SD		0.9	4.7	3.2		1.0	5.2	3.6
Spring 2015	Minimum	144	−17.3	−129.6	−5.8	83	−16.7	−124.3	−5.8
	Maximum		−11.4	−96.8	10.6		−11.4	−96.8	10.6
	Range		5.9	32.8	16.4		5.4	27.5	16.4
	Average		−15.0	−115.8	4.3		−15.0	−115.5	4.3
	SD		0.9	4.7	2.8		1.0	5.3	3.2
Fall 2015	Minimum	139	−16.8	−125.1	−6.4	83	−16.8	−124.6	−6.4
	Maximum		−11.1	−95.2	10.1		−11.1	−95.2	10.1
	Range		5.8	29.9	16.5		5.8	29.4	16.5

[a]Statistics shown include average, standard deviation (SD), minimum, maximum, range, and number of sites (n). Values of $\delta^{2}H$, $\delta^{18}O$ and *d* are expressed in ‰ relative to Vienna Standard Mean Ocean Water (VSMOW).

Barth [2012] and *Good et al*. [2014b]. Accuracy and precision were checked throughout the period of analysis using laboratory reference waters; the analytical precision of the instruments used was within ± 0.20‰ and ± 0.04‰ for the hydrogen and oxygen isotopes based on the standard deviation of the mean calibrated PT values from runs conducted during the analysis period (April 2013 to October 2015).

2.4. Spatiotemporal Analysis

We analyzed data from fixed sites to identify those sites with common isotopic characteristics throughout the sampling period. Principal Component Analysis (PCA) was performed on the data set to remove the correlation among the variables. The analysis used *k*-means clustering, which splits the data set into *k* groups by maximizing between-group variation relative to within-group variation. Clustering was based on $\delta^{2}H$, $\delta^{18}O$ and deuterium excess ($d = \delta^{2}H - 8 \times \delta^{18}O$) values from all six surveys, and the groups were obtained using the Hartigan-Wong algorithm in R 3.2.2 [*R Core Team*, 2015].

Given the common modes of isotopic variation exhibited by sites within each cluster group, we evaluated the possibility that information on the isotope ratios and distribution of waters from each group could be used to predict the values that would be observed at "unsampled" locations within the SLV. For each cluster group (*c*) and each survey (*s*), we calculated the mean isotopic value $\left(\bar{\delta}_{c,s}\right)$. We then estimated the average tap water isotope value for each water district (*wd*) and each survey (*s*), defined as a weighted average of the mean values for each

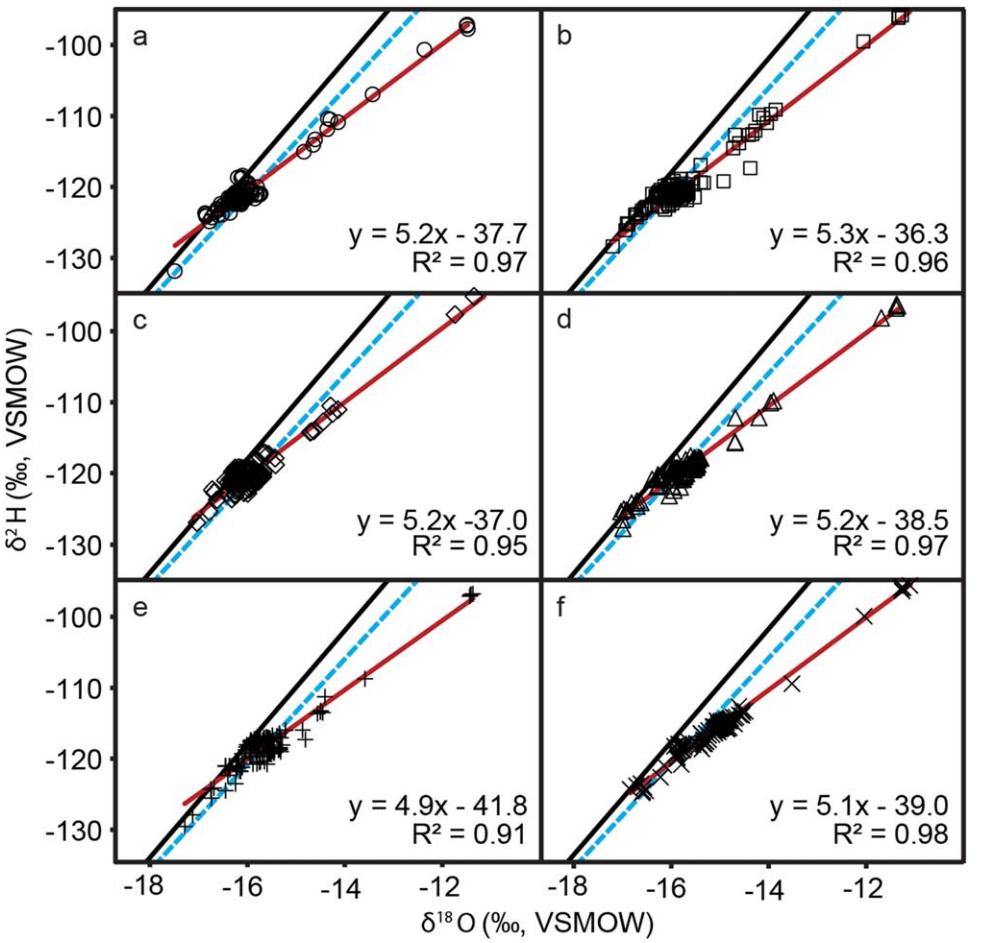

Figure 2. Isotopic composition of the tap water samples across the SLV metropolitan area. The black and the blue-dashed lines represent the global meteoric water line ($\delta^2H = 8 \times \delta^{18}O + 10$) and the local meteoric water line ($\delta^2H = 7.45 \times \delta^{18}O - 1.66$), respectively. The red lines and equation represent ordinary least squares best fits to data from each survey. (a) spring 2013, (b) fall 2013, (c) spring 2014, (d) fall 2014, (e) spring 2015, and (f) fall 2015.

cluster group represented within the district $\left(\bar{\delta}_{wd,s} = \sum((\bar{\delta}_{c,s}) \times n) \Big/ \sum n\right)$, where n is the total number of sites within a cluster group and $\sum n$ is the total number of sites in a water district. We tested these predictions against independent data from the intermittent sites, calculating residuals for each intermittent site measurement as the difference between the observed value and the calculated $\bar{\delta}_{wd,s}$ for a given district and survey.

We compared the mean of the isotope ratios (δ^2H and $\delta^{18}O$, paired t test) for the different surveys and calculated the spatial autocorrelation (Moran's I value) in the isotope ratios for the different surveys. We also estimated the mean water isotope ratios $\left(\bar{\delta}_{t,s}\right)$ of the total tap water flux (t) across the SLV for each survey period. We included all the sites (intermittent and fixed) in calculating $\bar{\delta}_{t,s}$. We began by calculating the isoflux $\left(\bar{\delta}_{wd,s,all}\ X\ Q_{wd,s}\right)$ for each district and each survey, using yearly water consumption data (Q_{wd}) available for 2014–2015 from the Utah Division of Water Rights website (water use publications, http://www.waterrights.utah.gov/distinfo/wuse.asp) to estimate district-specific value. The SLV-wide isoflux was calculated as the sum of the isofluxes of all the districts, and was divided by the total water use across the SLV to obtain the valley-wide mean tap water isotopic composition $\left(\bar{\delta}_{t,s} = \sum((\bar{\delta}_{wd,s,all}) \times Q_{wd,s}) \Big/ \sum(Q_{wd,s})\right)$. All statistical calculations were performed in R 3.2.2 [*R Core Team*, 2015] and maps were plotted using ArcGIS 10.2 (ESRI; Redlands, CA). Last, we explored possible correlations with data obtained from the United States Census Bureau, including population and median household income, which we aggregated for each municipal district and water district.

3. Results

Across all surveys, the stable isotope ratios of SLV tap waters ranged from −131.9 to −95.2‰ for δ^2H (average = −118.0‰, SD = 5.0‰) and from −17.5 to −11.1‰ for δ^{18}O (average = −15.6‰, SD = 1.0‰). The distribution of δ values is similar for all the surveys across the three years, and is nonnormal, multimodal, and positively skewed for both elements. A majority of the tap water data from the first five surveys were situated within 2‰ (for δ^2H) of the Local Meteoric Water Line, as defined by precipitation data collected during the 2013–2015 period (LMWL, $\delta^2H = 7.45 \times \delta^{18}O - 1.7$, $R^2 = 0.98$), with a small subset of samples (16%) falling well below the LMWL (Figure 2). For fall 2015 survey, a larger fraction of the samples (63%) fell at least 2‰ below the LMWL (Figure 2). Deuterium excess values, which decrease as evaporative losses from soils and surface waters increase, ranged from 10.9 to −5.5‰ (average = 6.4‰). We fit a local evaporation line (LEL) to the data from each survey and found that slopes for all surveys were similar and between 4.9 and 5.3. These slopes are comparable to that of the LEL (slope = 5.2) observed for evaporating surface waters collected in the region [*Nielson and Bowen*, 2010].

The unweighted average δ^2H and δ^{18}O values for the entire SLV (fixed and intermittent sites combined) varied between the different survey periods (Table 2). Overall, we noted a positive trend in the isotope ratios during the survey period, with average values for the SLV increasing by more than 4 and 0.9‰ for δ^2H and δ^{18}O. The SLV tap water samples showed a large but consistent isotopic range (~ 30‰ and ~6‰ for δ^2H and δ^{18}O) for all the different surveys. Intradistrict isotopic ranges were smaller and were also similar among the different surveys, with the average intradistrict range (for districts with > 5 sites) varying between 1.0 and 3.0‰ for δ^2H and between 0.2 and 0.5‰ for δ^{18}O. Statistical tests based on data from fixed sites only support these patterns. Differences in the average δ^2H and δ^{18}O values between most of the different surveys were statistically significant (paired *t* test for means, $p < 0.05$, Table 3). No significant differences in the variance for δ^2H, δ^{18}O and *d* were detected across the different surveys (F test for variance, $p > 0.05$).

Tap water δ^{18}O values exhibited weak spatial autocorrelation for all surveys (Moran's I value for spring 2013 through fall 2015 = 0.14, 0.24, 0.24, 0.17, 0.21, and 0.27, Z = 4.5, 6.5, 7.7, 6.5, 6.4, and 8.4, for all $p < 0.05$). Similar spatial correlation was observed for δ^2H and *d*. Samples collected on the eastern side of the SLV tended to have slightly lower δ^2H and δ^{18}O values compared to those collected on the western side (Figure 3). The highest isotopic values (> −100‰ and > −12‰ for δ^2H and δ^{18}O) were consistently observed on the northwestern side of the valley and the lowest values for each sampling event were observed on the eastern side of the valley (< −120‰ and < −16‰ for δ^2H and δ^{18}O). In general, sites situated close to each other (ground distance < 0.2 km) and falling within the same water district tended to have similar isotopic ratios, but adjacent sites straddling boundaries between some (but not all) water districts showed substantial differences (Figure 3). Large differences at closely situated sites were infrequent, but were consistently observed between

Table 3. Results of Paired t-Tests for Isotopic Data From the Surveys[a]

	δ^{18}O		δ^2H	
	Mean of the Differences	*p*-Value	Mean of the Differences	*p*-Value
Spring 2013 to Fall 2013	−0.24	<0.05	−0.54	0.13
Spring 2013 to Spring 2014	−0.18	<0.05	−1.31	<0.05
Spring 2013 to Fall 2014	−0.31	<0.05	−1.37	<0.05
Spring 2013 to Spring 2015	−0.32	<0.05	−2.11	<0.05
Spring 2013 to Fall 2015	−0.87	<0.05	−4.27	<0.05
Fall 2013 to Spring 2014	0.06	0.21	−0.75	<0.05
Fall 2013 to Fall 2014	−0.05	0.25	−0.82	<0.05
Fall 2013 to Spring 2015	−0.07	0.22	−1.56	<0.05
Fall 2013 to Fall 2015	−0.62	<0.05	−3.72	<0.05
Spring 2014 to Fall 2014	−0.11	<0.05	−0.07	0.78
Spring 2014 to Spring 2015	−0.14	<0.05	−0.81	<0.05
Spring 2014 to Fall 2015	−0.68	<0.05	−2.97	<0.05
Fall 2014 to Spring 2015	0.02	0.62	−0.73	<0.05
Fall 2014 to Fall 2015	−0.57	<0.05	−2.89	<0.05
Spring 2015 to Fall 2015	−0.54	<0.05	−2.15	<0.05

[a]Values of δ^2H and δ^{18}O are expressed in ‰ relative to Vienna Standard Mean Ocean Water (VSMOW).

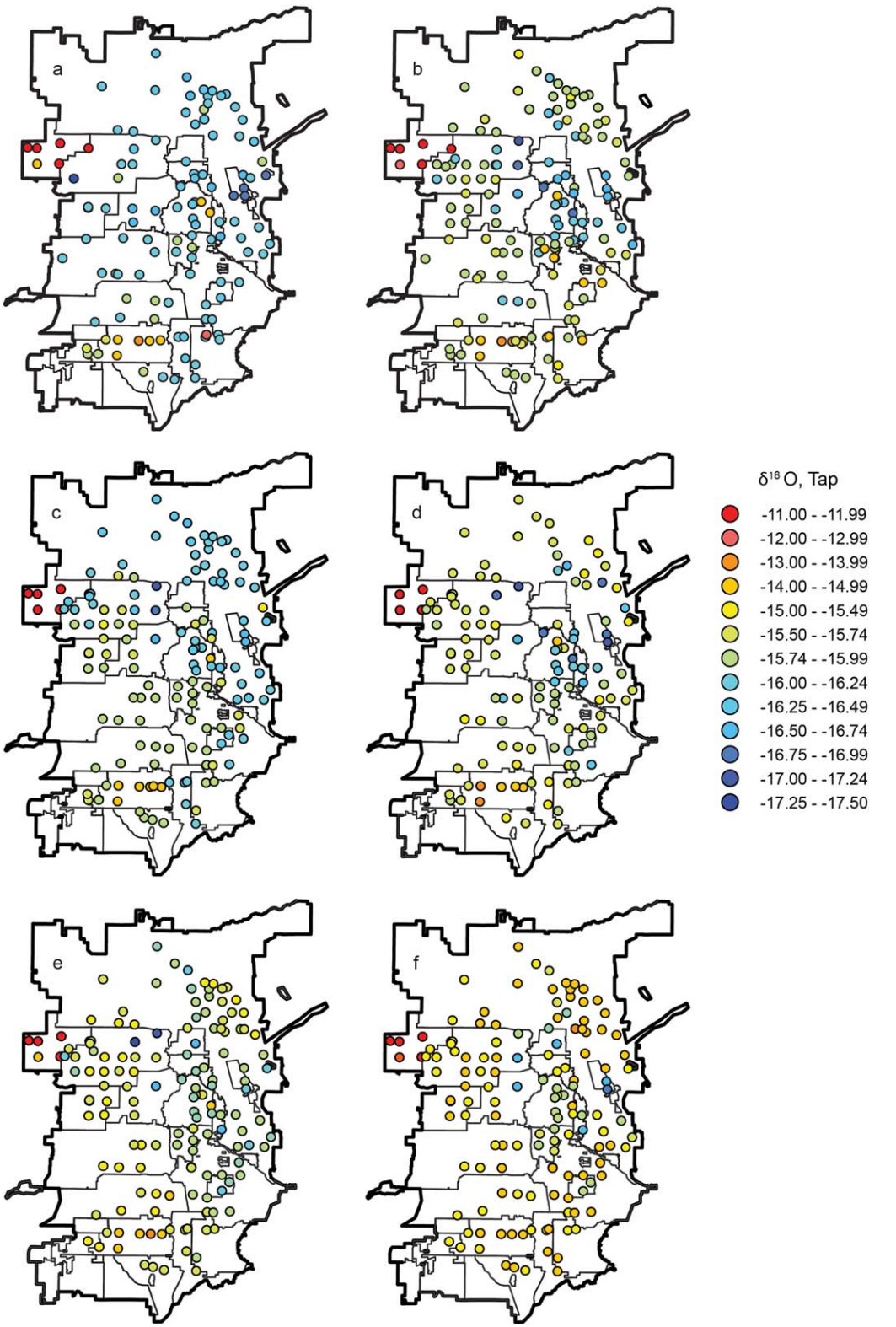

Figure 3. Observed $\delta^{18}O$ of tap water samples (intermittent and fixed sites) collected across the SLV. (a) spring 2013, (b) fall 2013, (c) spring 2014, (d) fall 2014, (e) spring 2015, and (f) fall 2015. All values are in ‰ relative to VSMOW.

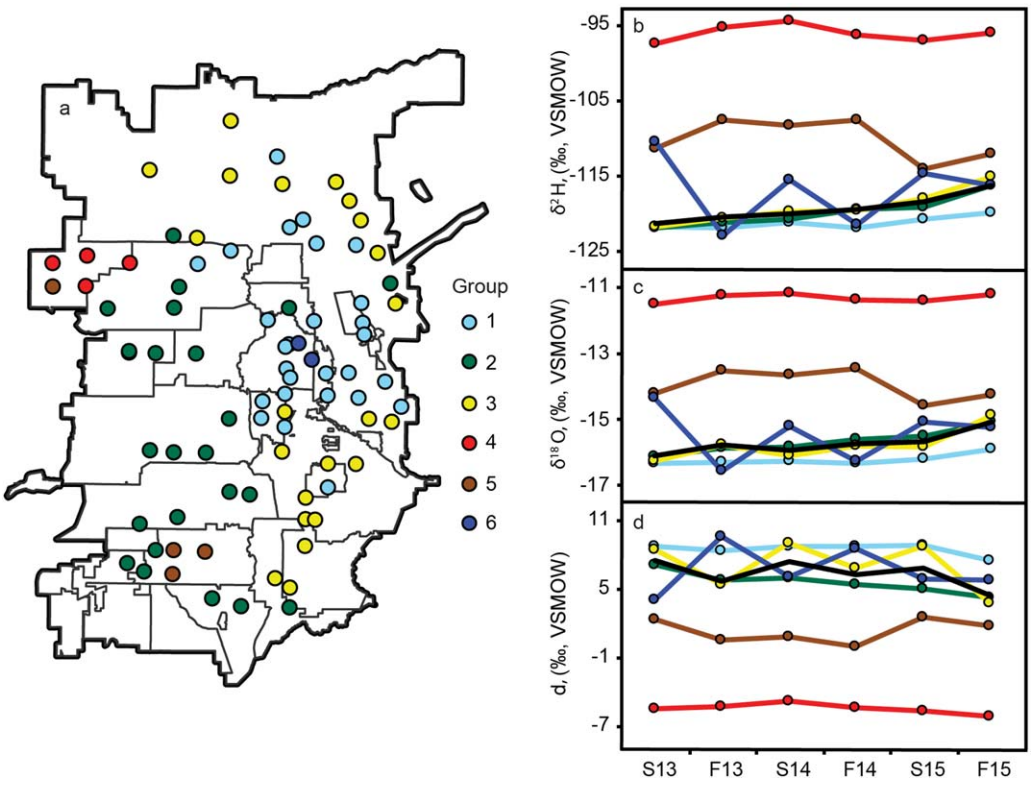

Figure 4. Spatial distribution of isotope cluster groups (a), their mean isotopic ratios (b-c) and D-Excess (d) for the six surveys. Black lines in Figures 4b–4d represent the consumption-weighted, regional average values for the entire SLV. All values are in ‰ relative to VSMOW. S13: spring 2013, F13: fall 2013, S14: spring 2014, F14: fall 2014, S15: spring 2015, and F15: fall 2015.

two sites (sampled within 500 m of each other) straddling the boundary of the Granger-Hunter and Magna water districts. Isotopic differences between these sites were more than 12‰ and 4‰, for δ^2H and δ^{18}O, during all the surveys (Figure 3).

4. Discussion

4.1. SLV Tap Water Cluster Group Patterns

K-means clustering divides the fixed sites into six groups, with 27, 24, 22, 4, 4, and 2 sites per group (Figure 4a). The majority of the sites (73 out of 83) are assigned to three main groups. With a few exceptions, the groups exhibit strong spatial clustering within the SLV, indicating that proximal sites tend to be characterized by similar tap water isotope ratios and patterns of temporal variation (Figure 4a). Sites belonging to groups 1 and 3 are clustered together in the eastern and northeastern parts of the valley (Figure 4a), with group 1 sites exhibiting a higher density in the east-central valley and group 3 being more concentrated in the northern and southern extremes of this region. The other major group, group 2, dominates a swathe of the southern and western valley (Figure 4a) with only a handful of sites impinging on the areas dominated by groups 1 and 3. Groups 4 and 5 are clustered in two small, distinct regions and with the exception of one site classified with group 5 (discussed below) each of these groups is constrained to and dominates a single municipal water district. Group 6 constitutes a pair of sites clustered within the group-1-dominated region in the eastern side of the valley.

The coincidence of the group 4 and 5 distributions with water district boundaries, as well as the general—if imperfect—alignment of the boundary between the regions dominated by group 2, and groups 1 and 3 with north-south water district boundaries throughout the central valley, suggests that the role of these districts in brokering and managing water supplies used by their residents is reflected in the spatiotemporal distribution of tap water isotopes ratios. However, the larger-scale clustering of sites categorized within the major groups also suggests a higher order of organization within the regional water distribution system.

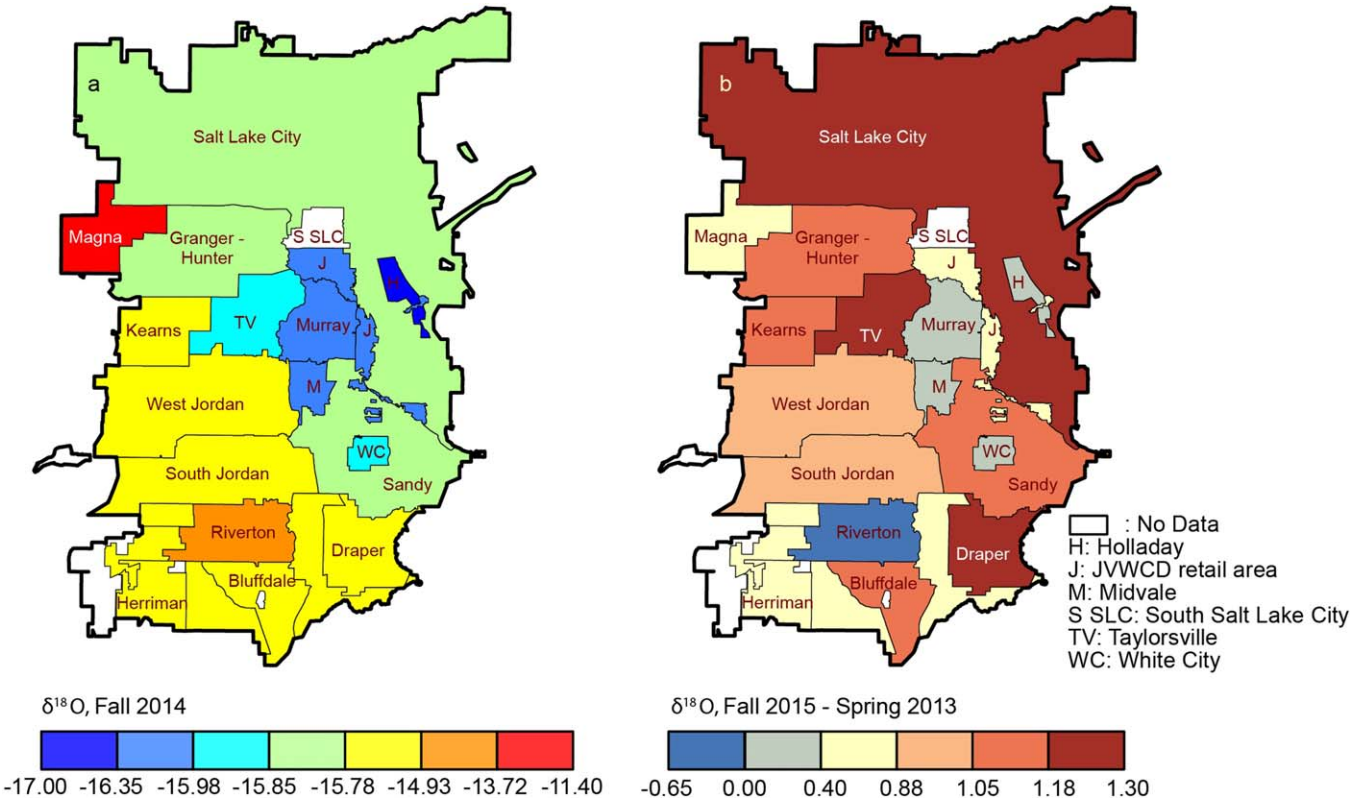

Figure 5. Example district average water isotope metrics. (a) District average δ ^{18}O values for tap waters collected across SLV in fall 2014. (b) Difference in the district average δ ^{18}O values of tap waters between fall 2015 and spring 2013. All values are in ‰ relative to VSMOW. Color scale boundaries were determined based upon geometric breaks in the data.

Indeed, the distribution of group 2 and group 3 sites approximates the service regions of the two major regional wholesalers, the JVWCD and MWD, respectively. Specific links between water sources, management practices, and the tap water isotope ratios will be discussed in subsequent sections, but the spatial association of the data with the footprint of management districts and wholesaler service areas itself provides an indication that the isotopic data reflect aspects of the structure of the water distribution system.

The average isotope ratios of tap waters in each of the management districts also demonstrate strong geographic variation in values across the SLV. The average isotopic composition is lower in the districts on the northern and the eastern sides of the valley compared to the districts on the western and southern sides (Figure 5a), with distinct pockets of lower or higher values occurring in several districts in the valley center and the Magna and Riverton districts. These spatial patterns do not follow climatic, hydrological, or natural isotope gradients [*Thiros and Manning*, 2004] within the SLV, again highlighting the role of water management in governing the patterns we observe. Despite the spatial heterogeneity of the data, however, values from every district except one (Riverton) show a common temporal trend toward higher isotope ratios over the 3 year sampling period (Figure 5b). This overarching trend suggests a third level of control on the tap water isotope data: regional environmental influences on the isotopic composition of water sources used across the SLV.

4.2. Cluster Group Water Source Signatures

Water isotope data from the six groups are distinguished from each other both by absolute values and by short-term (intra-annual) and long-term (interannual) temporal variation. These three diagnostic modes of variation can be linked to water source. The following section describes these and other features of the data set that can be used to infer characteristics of the water sources in different parts of the SLV. Although specific information on the sources of water to individual sample sites was not available in our study, the isotopic characteristics of different groups can be used to infer source information that can be compared with general reporting data on sources used by SLV water districts.

Table 4. Average, Standard Deviation, and Average Difference Between Spring and Fall Isotope Ratios for Different Cluster Groups Within the SLV Across the Entire Study Period[a]

	Average			Standard Deviation			Average Fall to Spring		
Group	$\delta^{18}O$	$\delta^{2}H$	*d*	$\delta^{18}O$	$\delta^{2}H$	*d*	$\delta^{18}O$	$\delta^{2}H$	*d*
1	−16.2	−121.2	8.5	0.2	0.8	0.5	0.1	0.0	−0.6
2	−15.7	−119.7	5.6	0.4	2.0	1.0	0.3	1.6	−0.9
3	−15.8	−119.0	7.1	0.5	2.3	2.1	0.6	1.4	−3.4
4	−11.3	−96.0	−5.4	0.1	1.1	0.4	0.1	0.5	−0.3
5	−13.9	−110.1	1.4	0.5	2.7	1.1	0.4	2.2	−1.1
6	−15.4	−116.8	6.7	0.8	4.6	2.0	−1.2	−6.6	2.7

[a]Values of $\delta^{2}H$, $\delta^{18}O$ and *d* are expressed in ‰ relative to Vienna Standard Mean Ocean Water (VSMOW).

4.2.1. Low-Variance Groups

Groups 1 and 4 are distinguished by their relatively invariant values across the 3 year sampling period (1 standard deviation for group mean $\delta^{18}O$ values $<0.15‰$, average fall-spring $\delta^{18}O$ difference $<0.1‰$; Table 4; Figures 4b–4d). Although it is possible that multiple isotopically distinct or varying sources were used to supply the sites constituting these groups, and that the source blend changed in a way that maintained a constant tap water composition, a more parsimonious explanation is that water was supplied to these sites from an isotopically invariant source. Unlike surface water resources, which are affected by strong seasonal variation in precipitation water isotope ratios and runoff sources, isotopic values for groundwaters tend to exhibit limited seasonal and highly damped long-term variability [*Clark and Fritz*, 1997; *Wassenaar et al*., 2009]. We thus interpret the data from groups 1 and 4 as indicative of groundwater-dominated supply regions. Isotopic values observed in group 1 are similar to those measured for regional deep groundwaters in the aquifers underlying the eastern part of the valley [*Thiros*, 2003; *Thiros and Manning*, 2004], and reporting data from the water districts supports our interpretation that wells tapping these aquifers constitute a large part of the water supply to this area (http://www.murray.utah.gov/DocumentCenter/Home/View/1313, http://www.midvalecity.org/dp.aspx?p=65). Indeed, tritium and helium-3 dating suggests the mean age of groundwater within the SLV to be approximately 15 years, indicating a relatively long-residence time consistent with the lack of preservation of seasonal $\delta^{2}H$ and $\delta^{18}O$ trends observed in our surveys [*Thiros*, 2003]. Values for group 4 samples, in contrast, are the highest observed in our data set, and the high isotope ratios and low D-excess values for these samples are consistent with groundwater recharged at least in part by sources that had experienced substantial evaporation. The values we measured from taps in this area are consistent with those previously reported for public supply wells constituting the primary water source for the Magna Water District [*Thiros and Manning*, 2004]. Measurements for these wells and for other subsurface waters sampled in this part of the SLV show high sodium and chloride ion concentrations [*Thiros and Manning*, 2004], consist with our inference of a distinct, evapoconcentrated recharge source.

4.2.2. Seasonal Groups

Isotope data from groups 2 and 3 exhibit variability characterized by seasonal oscillation superimposed on a trend of increasing $\delta^{2}H$ and $\delta^{18}O$ through the study period (Figure 4). Overall variance in the mean values of groups 2 and 3 is larger than in groups 1 and 4. For both groups (2 and 3), H and O isotope ratios for the fall sampling periods are higher and *d* values lower, than for the corresponding spring periods (Table 4). This seasonal pattern is stronger for group 3 sites than for group 2. Within group 2, the data are arrayed along a line in $\delta^{2}H/\delta^{18}O$ space that lies below the local meteoric water line (Figure 6b) and within group 3 the data show large seasonal variability with values lying above the LMWL in spring and lying on or below the LMWL in fall (Table 4, Figure 6c). These tap water lines exhibit slopes of 5.4 and 4.3 for groups 2 and 3, respectively, which are similar to previously observed surface water evaporation line slopes in the region [*Kendall and Coplen*, 2001; *Dutton et al*., 2005; *Nielson and Bowen*, 2010] and suggest that variation in evaporative water loss drives much of the isotopic variation observed in tap water from these groups.

As groundwaters are isolated from seasonal evaporation, we interpret groups 2 and 3 to represent tap waters sourced primarily from one of the two surface water sources employed in SLV. Water production data indicates that approximately 60% of water used in the SLV is extracted from surface waters (water use publications, http://www.waterrights.utah.gov/distinfo/wuse.asp). Further, the districts supplying waters to the areas with sites in group 2 and 3 are the known service areas of districts supplying water from the JVWCD and MWD, respectively. Comparison of the isotopic characteristics of group 2 and 3 waters suggests

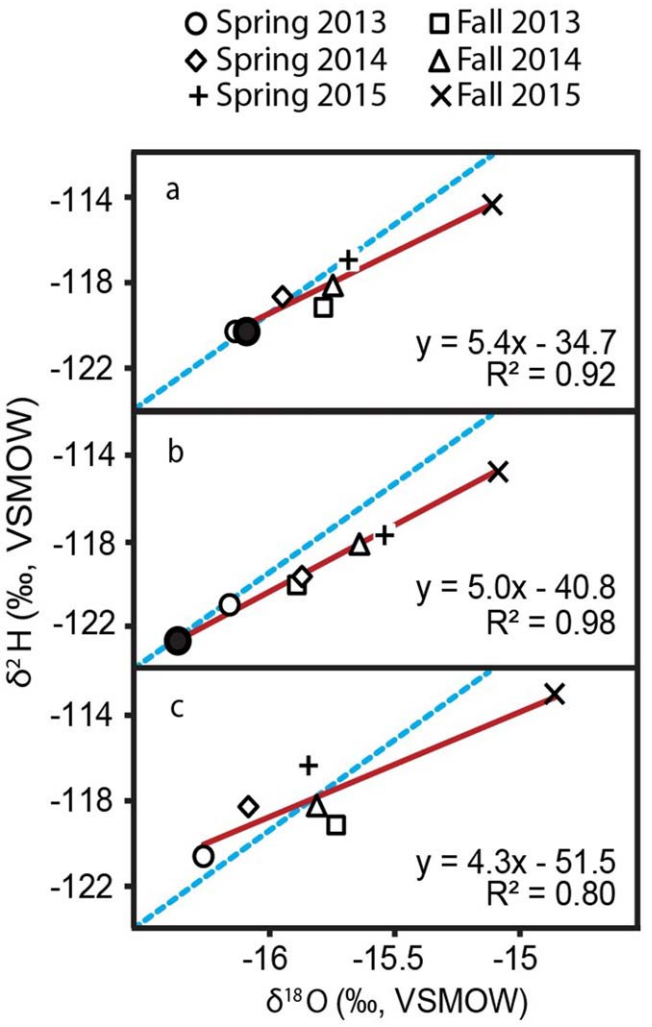

Figure 6. Evaporative trends in SLV tap waters across the 3 year sampling period. Values shown are consumption-weighted SLV-wide means (a) and mean values for cluster groups 2 (b) and 3(c). The blue-dashed line in each plot is the LMWL and the red line is the best fit line to the data, representative of the local evaporation line (LEL). Filled black circles in Figures 6a and 6b show inferred preevaporation source water isotopic compositions estimated by the intersection of the LEL and LMWL.

that the data may document nuances reflecting differences in these two major surface water systems. The lower variability and incredibly tight correlation of group 2 water values along an apparent evaporation line (Figure 6b) is consistent with waters from these sites being derived dominantly from a single surface water system having a relatively large storage capacity and long turnover time. Extraction from the Provo River system constitutes the majority (65%) of the water supplied by JVWCD (2014 Annual report, https://jvwcd.org/public/highlights). Although we were not able to estimate a system-wide turnover time, the Provo River system includes two large (capacity: 448 $\times$ 10^6 m^3 and 188 $\times$ 10^6 m^3) and numerous small reservoirs, harvests water from a large catchment area ($\sim$1500 km^3), and is operated as a major source year-round.

In contrast, the greater variability of the group 3 data about their evaporation line (Figure 6c) suggest derivation from a more isotopically "volatile" source and/or more dynamic use of multiple water sources to supply taps in this group. Indeed, the smaller storage capacity of the multiple Wasatch creek systems managed by MWD should translate into lower transit times and greater isotopic variability of these sources. The seasonal nature of runoff from Wasatch creek [*Bardsley et al.*, 2013] watersheds mean that MWD and their client districts supplement water from these sources with water from the Provo River system during low-flow seasons (http://www.mwdsls.org/pdfs/Annual_Report_2014_ Final.pdf). We note that isotopic values of group 2 and 3 sites converge, in general, during the fall sampling events, consistent with a convergence of water sources across the region during the fall low-flow period.

4.2.3. High Variance Groups

Groups 5 and 6 are characterized by substantial isotopic variation over the study period, but exhibit temporal patterns of variation that are distinct from those of the "seasonal" groups. In addition, data from these small groups have much higher within-group variance than seen for groups 1–4 (e.g., for $\delta^{18}O$ the average within-group standard deviation for a given sampling period is 0.94 and 0.75‰ for groups 5 and 6, respectively, and $<$0.38‰ for all other groups). Isotopic data for sites within each of the high variance groups exhibit some common features, but do not follow a single, uniform trend (Figure 7).

Sites within cluster group 5 show two distinct patterns of variation that map onto the geographic distribution of these sites. Tap water isotope ratios for three sites within the Riverton water district are relatively stable or decline slightly over the first 2 years of sampling and then drop by $\sim$1‰ over the final year of sampling (Figure 7a). During the final sampling event (fall, 2015), the values at these sites are

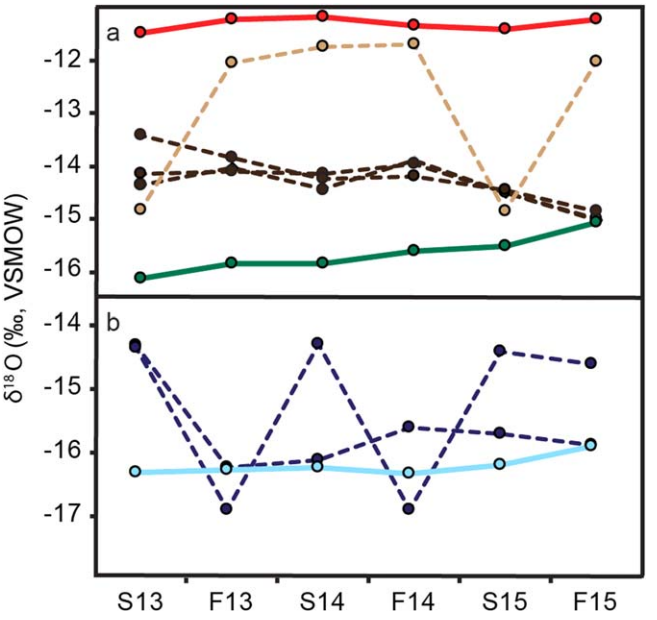

Figure 7. Isotopic data for high-variance cluster groups. (a) $\delta^{18}O$ values for group 2 (green), group 4 (red), and individual sample sites of group 5 (light and dark brown dashed lines; light = Magna, dark = Riverton). (b) $\delta^{18}O$ values for group 1(light blue) and individual sites of group 6 (dashed dark blue lines).

indistinguishable from those of the cluster group 2 sites. This distinctive pattern of isotopic variation is not easily reconciled with expected climatic or hydrological variation in a single water source, suggesting a shift in the water sources used to supply these sites. In fact, the Riverton City water utility phased out production from its local City wells during 2015, and by our final sampling event was providing water purchased from JVWCD (http://www.rivertoncity.com/waterutility.culinary.html). Data from the other group 5 site, situated within the Magna Water District, show a unique pattern of discrete isotopic variation across the six sampling events (Figure 7a). Values for all sampling events at this site fall on a mixing line between average values for the two other cluster groups occupying this part of the SLV (groups 2 and 4; Figure 8). Although we do not have access to source data specific to this site, we suggest that the isotopic data likely indicate that a varying blend of Magna City well and JVWCD wholesale water was supplied to this part of the Magna Water District over the 3 years of sampling. The six isotopic measurements from this site group tightly into three pairs, providing some suggestion that water managers were using a limited number of preferred blending ratios (approximately 20%, 80%, and 90% Magna well water) to produce the water mixtures.

Data from the two sites comprising group 6 exhibit irregular fluctuations between low values similar to those of the east-SLV groundwater-dominated cluster group (group 1) and a second set of values characterized by higher isotope ratios and lower D-excess values (Figure 7b). We have limited information on water management within the Murray Water District, but public reports suggest that water is locally sourced from a large number of springs and wells (http://www.murray.utah.gov/DocumentCenter/Home/View/1313). All 12 data from the group 6 sites fall tightly on a line in $\delta^{2}H$-$\delta^{18}O$ space with a slope of 5.5 ($r^2 = 0.996$), consistent with use of water with a uniform initial isotopic composition but subject to varying degrees of evaporation. We therefore suggest that the isotopic data likely reflect use of multiple groundwater systems bearing water that experienced differing degrees of evaporation prior to recharge. Previous work on public supply wells has documented a wide range of recharge modes for groundwaters within this part of the SLV, such as subsurface inflow from mountain blocks, infiltration from mountain-front streams, and infiltration of excess irrigation and lawn water [*Thiros and Manning*, 2004;

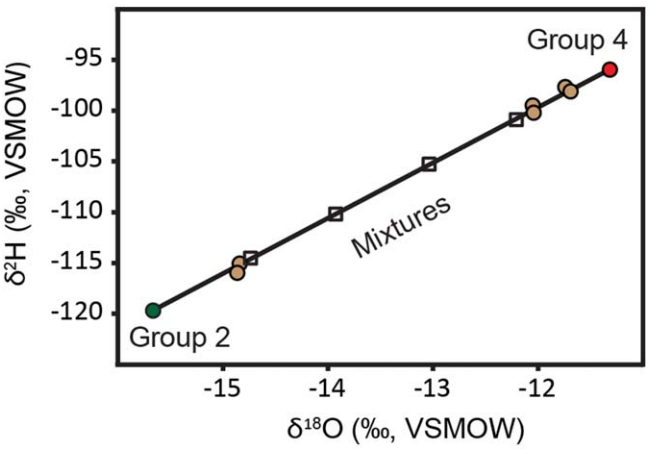

Figure 8. Mixing relationship for waters collected at the group 5 site (light brown-filled circles) in the Magna water district. Green and red-filled circles show the long-term mean isotope ratios for group 2 and group 4 tap waters. The mixing line (black line) between these endmembers is marked with open black squares showing 20, 40, 60, and 80% contributions from the different groups.

Bexfield et al., 2011], but not the wide range of isotopic compositions measured here for group 6 tap waters.

The ability to distinguish and map the structure of the water distribution system with water isotopes, and to establish connections between taps and climatic water sources, could support numerous applications. In areas with diverse water sources and complex networks of public and private stakeholders, the tools developed here could support monitoring and enforcement of water rights. Information connecting water sampled within distribution systems or at the point of use to environmental sources could be valuable in evaluating the susceptibility of these waters to climatic changes or water quality impairment (e.g., as exemplified by the contrasting susceptibilities of water from surface or fossil groundwater sources). In addition, information on connectivity within distribution systems could be of use in tracking of contaminants and nonconservative tracers introduced within the system itself and response to critical water contamination events.

4.3. Long-Term Isotopic Trend

The waters available to the growing population of SLV are sensitive to seasonal climate dynamics. The 2013–2015 period featured above average temperatures and below average precipitation across the SLV and adjacent watershed areas, with the last above-average water year occurring during 2011 (Table 1). These factors should significantly affect the δ^2H and δ^{18}O values of SLV tap waters. Our estimate of the SLV-wide water isotope budget gives mean tap water isotope ratios of $-121.3‰$ and $-16.1‰$ (δ^2H and δ^{18}O) in spring 2013 and suggests a nearly monotonic increase for δ^2H and an increasing trend with a superimposed seasonal oscillation for δ^{18}O during the subsequent samplings (Figures 4b and 4c). The overall increase in mean tap water isotope ratios is more than $5‰$ and $1‰$ for δ^2H and δ^{18}O, respectively, between 2013 and 2015. Average values for the individual surveys lie along a line of slope 5.0 ($r^2 = 0.92$), suggesting that the evolution in basin-wide tap water isotope ratios over the course of the study period may reflect trend toward increasing evaporative water loss with time. We suggest that the combination of below-average recharge of reservoirs and above-average evaporative demand may have driven a progressive increase in evapoconcentration of surface water resources supplying the SLV. Based upon our data, it is difficult to constrain weather the isotopic enrichment is due to elevated temperature and/or due to below average precipitation in the region.

To understand the impacts of these climate dynamics on SLV water supply, we estimate the total evaporative loss from watersheds, reservoirs, and distribution systems employed by districts in SLV using the modified Craig-Gordon (C-G) model [*Craig and Gordon*, 1965; *Skrzypek et al*., 2015]. The model requires initial and postevaporation values of the stable isotope composition of the water pool and estimated values for the stable isotope composition of moisture in the ambient atmosphere, atmospheric temperature, and humidity. For our analysis, the initial source water value was estimated by projecting the evaporation line defined by the consumption-weighted average tap water isotope data back to the SLV LMWL ($-120.6‰$ and $-16.0‰$ for δ^2H and δ^{18}O, respectively, Figure 6a). The isotopic composition of the ambient air moisture was estimated using the methods described in [*Gat*, 1995], [*Gibson and Reid*, 2014], and [*Gibson et al*., 2016]. We used mean annual temperature and humidity values from Salt Lake International Airport (http://www.ncdc.noaa.gov/IPS/cd/cd.html; T = 12.4, 12.4 and 13.7°C, RH = 0.52, 0.51, and 0.51 in 2013, 2014, and 2015, respectively), which were intended to provide only a rough approximation of the conditions within the SLV water source region during warm-season periods when the majority of evaporation occurs [*Gibson et al*., 2008, 2016]. We used the kinetic fractionation factors appropriate for open-water evaporation in a continental environment [*Vogt*, 1976]. Although some fraction of the evaporation recorded in the tap water data may have occurred within soils of the SLV water supply watersheds, recent studies suggest that soil evaporation has a limited effect on the isotopic composition of groundwaters and streams [*Evaristo et al*., 2015; *Good et al*., 2015]. Our calculation suggests that evaporative losses from the SLV water supply increased from 1 to 1.5% of the total water flux in 2013 to 4 to 6% in 2015. Using yearly water consumption data for the SLV obtained from the Utah Division of Water Rights website (see section 2.4), these values translate into >15,000 m^3 of evaporative loss per day in 2015 (assuming a conservative loss rate of 4%). This enhanced loss to the atmosphere would equate to $2.25 million of revenue loss in 2015 (calculated at current rates of $1.16 per unit within Salt Lake City; 1 unit = 2.83 m^3) if translated into reduced extractions, or significant ecological impacts if extraction remained unchanged.

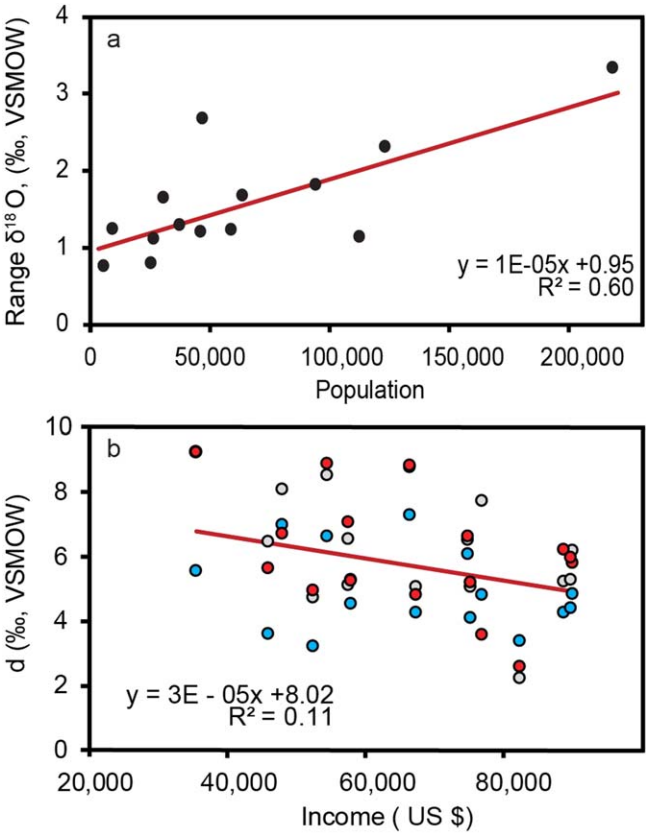

Figure 9. Comparison of tap water isotope metrics with select socioeconomic data. (a) Correlation between water district population and the range of observed $\delta^{18}O$ values (Magna and Murray districts not included). (b) Correlation between district average per household annual income and average tap water D-Excess value (Magna not included). Red, blue, and grey circles represent fall 2013, fall 2014, and fall 2015, respectively. Regression line includes data from all the 3 years. All regressions are statistically significant ($p < 0.05$).

The evapoconcentration trend observed within the SLV-wide, consumption-weighted data is even more strongly expressed in data from cluster group 2, which is interpreted to primarily record values from the highly impounded Provo River System. C-G calculations for data from this group, using meteorological values estimated from measurements at Deer Creek Reservoir (T = 6.5, 8.0, and 8.4°C in 2013, 2014, and 2015; RH = 0.50 for all years), suggest evaporative losses of 2–2.5%, 3.5–5%, and 5.5–8% in 2013, 2014, and 2015. The Provo system has a multiyear turnover time (at least 1.3 years, estimated considering only the ratio of Provo River inflow to the capacity of the two major reservoirs within the system), and the enhanced accumulation of evaporative influence over the multiyear climatic anomaly of the study is not surprising in this context.

Although the calculations presented here are simple first-order estimates, and could be refined with the collection of additional field data to better constrain model parameters, they indicate the potential to reconstruct dynamic changes in evaporative water loss from large-scale water supply systems and quantify these losses as a component of the water budget of a major metropolitan region. The data suggest that during a 3 year period of drier and warmer than average climate these losses accelerated and accumulated, removing an additional 9400 m^3 to 11400 m^3 of water per day from the SLV public supply system at the end of 2015 relative to the beginning of the study period.

4.4. Demographic Associations

Because the water supply system of the SLV has been developed over time to provide reliable water distribution to a dispersed and evolving population, we anticipate that the isotope data, reflective of the sources of water used, may reveal different patterns and strategies of water supply management that correlate with variation in demographic characteristics of SLV communities. We observe significant positive correlation between the range of isotope ratios for all tap water samples collected in a given water district (calculated as the difference between maximum and minimum isotope ratios observed in the district over the entire sampling period) and the population of that district (Figure 9a). The largest isotopic ranges occur in Granger-Hunter and Salt Lake City, the two districts with the highest population. Low ranges are observed for smaller districts such as Midvale, Holladay, and Bluffdale. Given the association between water source type and isotope values introduced in section 4.2, this correlation may reflect the tendency for larger districts to use water from multiple sources to meet their higher water demands. Similar relationships have been reported on a national scale: 70% of hydrological basins with population less than 100,000 inhabitants rely only on single source of water, whereas basins with large population, particularly in water-limited regions such as the southwestern United States, commonly rely on multiple sources and nonlocal water [*Fort et al.*, 2012*; Landwehr et al.*, 2014]. A recent isotope-based analysis of water use across the western

United States has shown population to be a significant predictor of nonlocal water use [*Good et al*., 2014a]. The reliance of districts with large population on multiple sources of water has implications for the resilience of these districts under situations of water scarcity. Importing water from an external source can be beneficial under scenarios of local water shortage; however, it may increase exposure to regional or extralocal drought.

Initial development of the SLV occurred at the northeastern edge of the basing along the base of the Wasatch Mountains in and around Salt Lake City (SLC). Later development led to westward and southward expansion of the urbanized area. Historic rights to water from the Wasatch creeks are allocated to many stakeholders within the SLV, but center on the cities of SLC and Sandy. Some cities with a later urbanization history, such as Midvale and Murray, used groundwater to cater its population. With the increase in the demand for water due to increasing population, the Provo River system was developed and used to source water for most of the cities in the south and west of the valley.

We observe a weak yet significant negative correlation between average income of SLV municipal districts and the average D-excess values of fall season tap water (Figure 9b). This relationship is not apparent during the spring season. Given the association of low fall-season deuterium excess values with surface water evaporation, as noted above, we hypothesize that the observed relationship indicates greater surface water consumption in districts with higher per-household income. This may reflect the geographic and historic structure of the urban area, as described above, where many of the affluent areas are situated in closer proximity to mountain surface sources and within areas of earlier development that often retain historic allocations of surface water rights. Another possible explanation may be the selective use of higher-quality surface waters by water managers in more affluent districts or the relative preference of wealthier community to develop in regions catered by surface waters. Given that majority of the SLV groundwater wells are located in and around the basin center, we consider the former, circumstantial possibility to be more likely.

4.5. Implications: Future Water Management

The population of the SLV is anticipated to double over the next 40 years (http://governor.utah.gov/DEA/demographics.html), and the resultant demands on water resources promise to be a significant challenge to sustainable development of this semiarid basin. Our isotopic assessment highlights several aspects of the municipal water systems supplying the SLV that are germane to planning for and understanding these future water resource challenges. First, our calculations show significant increase in evaporative losses within the system over the 3 year sampling period, likely attributable to the atypically warm and dry weather that persisted throughout the study. Given that majority of municipal water used within the SLV is currently sourced from surface water and the proposed development of water resources to satisfy future demands associated with population growth focuses primarily on surface water systems of the Central Utah Project and Bear River, SLV communities are and will continue to have strong exposure to changes in evaporative losses from these systems. Studies have projected a mean annual temperature increase of 1–3°C in the region by the mid-21st century, with stronger summer warming than winter [*Jardine et al*., 2013], and our data suggest that evaporative losses from existing SLV surface water supplies approaching 10% under these conditions could be plausible. Moreover, the isotopic data clearly show that short-term (year-to-year) climatic variability can have a significant impact on evaporative loss from water resources, detectable even at the scale of the entire SLV metro area. Historically, water managers have done a poor job incorporating the impacts of climatic variability in water resource planning [*Craig*, 2010], but as the gap between supply and demand narrows in this and other water-scarce regions, a greater recognition of variability, both in terms of inputs to hydrologic systems but also evaporative losses, will become increasingly important.

In addition, our data suggest that different parts of the SLV metro area may have different levels of exposure to future climatic variability and long-term change. Evaporative trends were weak or not detectable for sites within cluster groups 1 and 4, reflecting the damping of climatic variability by the groundwater systems supplying these sites. Although these sources may be more stable to fluctuations in hydroclimate, greatly increased extraction of groundwater in the SLV is unlikely to be sustainable. Groundwater extracted from the western part of the valley is of low quality and requires treatment, including reverse osmosis and ultra violet treatment, to make it fit for human consumption (www.itrcweb.org/miningwaste-guidance/cs48_kennecott_south.htm). Most of the groundwater wells in the valley exhibited an increase in the concentration of dissolved solids from 1988–1992 to 1998–2002, with some wells on the eastern side displaying

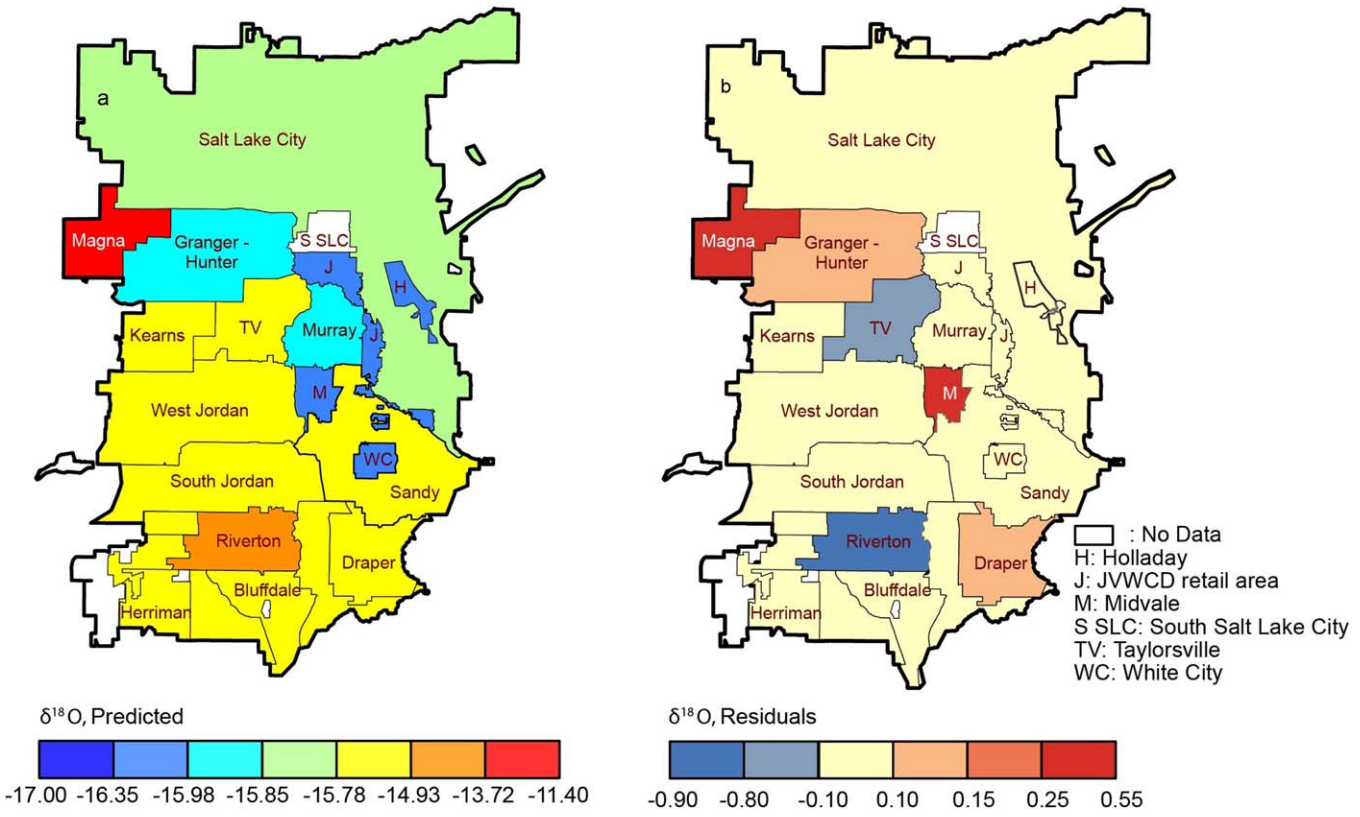

Figure 10. Predictive SLV tap water map and validation. (a) Estimated average SLV tap water $\delta^{18}O$ values for the study period based on cluster group isotope values and spatial distribution, as described in the text. (b) District average residuals calculated using data from intermittently sampled sites. All values are in ‰ relative to VSMOW.

an increase of more than 20%, likely due to lateral inflow of water with high solute concentrations from the western parts of the valley [*Thiros*, 2003]. Further, all the wells with modern water showed presence of anthropogenic compounds, suggesting human contamination [*Thiros*, 2003]. The low quality of groundwaters has already led some districts such as Riverton to migrate to surface water sources. Given that districts currently relying primarily on groundwater supplies are among the least affluent in the SLV, future declines in the stability of regional surface water sources and greater demand for groundwater could have significant impacts on local water markets and the balance of water rights "power" within the region.

4.6. City-Scale Tap Water Isotope Predictions

Isotopic signatures from environmental water sources are incorporated in plant and animal tissues [*Schoeller et al.*, 1986] and have been used to study wildlife migration, the geographic origin of foods, drugs and human remains, and in forensic analysis [*Hobson and Wassenaar*, 1996; *Hobson et al.*, 1999; *Ehleringer et al.*, 2008; *Chesson et al.*, 2010; *Bartelink et al.*, 2014]. These applications require knowledge of the geographic distribution and variation of water source isotope ratios [*West et al.*, 2010; *Kennedy et al.*, 2011], but human and product-focused applications have generally used regional or national-scale surveys and models of precipitation or tap water to guide interpretation of sample data. As demonstrated here and in a limited number of previous studies [*Williams*, 1997; *Kennedy et al.*, 2011; *Good et al.*, 2014a; *Landwehr et al.*, 2014], these regional assessments may not capture the local-scale variations in areas that rely on multiple water sources or import nonlocal water, potentially leading to interpretive bias or error or limiting the precision of geolocation analyses obtained using the isotopic data. Intensive city-scale sampling campaigns are labor-intensive and costly; however, the development of generalizable approaches to predict urban tap water isoscapes without onerous data overhead is desirable.

The data from our study provide spatially and temporally resolved documentation of city-scale variation in tap water isotope ratios that can be used both to evaluate the potential significance of this variation for forensic applications and to develop and test methods for urban tap water isoscape prediction. The

observed range and standard deviation (SD) of the isotope ratios in the SLV (intermittent and fixed sites combined) were greater than 30‰ and 4.5‰ for δ^2H, and 5.7‰ and 0.9‰ for δ^{18}O, respectively, for each sampling period. Although these values are consistent with estimates of local variability and predictive uncertainty derived from large-scale tap water studies [*Bowen et al*., 2007b; *Landwehr et al*., 2014], the new data elucidate important aspects of the structure of this variation that are not apparent in the large-scale studies. First, the data demonstrate that the majority of the variation within SLV tap water isotope ratios is spatial, rather than temporal, in origin, with most individual sampling sites exhibiting a minor range of values across the 3 year period relative to the range observed among sites. This suggests the potential for residents of subregions of the SLV to assimilate distinctive isotopic signatures from their local water supplies, although further work will be required to assess the degree to which movement of such individuals within the region and spatiotemporal averaging will diminish the actual expression of such signatures.

Second, our data document and characterize strong links between the spatial distribution of tap water isotope ratios and the water management systems of the SLV, providing a basis for modeling and prediction of local-scale water isotope patterns within the urban area. Most previous isoscape models for tap water have relied on natural spatial, climatic, or physiographic variables to predict water isotopic composition, but as our data demonstrate the spatial structure of isotopic variation within urban public supply systems is not necessarily determined by these variables. Based on our results, we adopt the SLV water management districts as our spatial map unit and estimate the long-term annual average tap water isotope distribution across the valley using information on cluster group isotopic values and distribution, as described in Methods. The resulting map (Figure 10a) shows the northeast-southwest trends across the valley which we previously attributed to use of different surface water sources, as well as pockets of distinct, higher, or lower values associated with localized groundwater use. As validation of the map, we calculated differences between the predicted water isotope values for each district and the observed values of tap water from the intermittently sampled sites situated within that district. These model residuals are normally distributed, with a standard deviation of 0.3‰ for δ^{18}O and a mean of 0.03‰. Large residual values ($>$ 0.5‰) occur primarily in the Magna and Riverton water districts (Figure 10b), where, as described above, temporal switching between isotopically distinct water sources was observed. For comparison, the standard deviation of residuals from these same sites when compared with the predictions of the national-scale model of *Bowen et al*. [2007b] is 1.0‰ for δ^{18}O, showing that substantial improvement results from incorporating information on the local water management system.

This analysis suggests the potential to characterize and accurately map the variation in tap water isotope ratios across a large urban center with fragmented and heterogeneous water management systems. Although the map presented here was based on a large number of physical samples, the approach may be generalized and applied in ways that maximize the predictive value of more limited physical sample data. In our workflow, the isotopic data were used both to identify the spatial structure of the water supply system and to characterize the isotopic composition of the water associated with different parts of that system (the cluster groups). In many cases, the entire workflow may not be dependent on collection of new sample data. To the degree that the structure of the SLV water supply system is static, for example, one could use limited, targeted sampling to characterize isotope ratios of waters associated with the already-defined cluster groups and create revised tap water isoscapes for future time periods. It is also possible that in many cities independent information on the structure of the water management system, along with limited sample data or models characterizing the isotopic composition of source waters, could be used to predict tap water isotope distributions without spatiotemporally intensive sampling at the point of use. In either case, attention to the potentially dynamic nature of both system structure/management (e.g., as seen for the Riverton water district during our study) and source water composition will continue to be warranted, as our data suggest that both factors drove perceptible changes in SLV tap water isotope ratios during our period of study.

5. Conclusions

Water isotopes have been used extensively to study natural components of the hydrological cycle over a wide range of spatial and temporal scales [*Gat*, 1996; *Bowen*, 2010], but their application to anthropogenically dominated urban water systems has been more limited. Here we demonstrate the expression of active

water management in the spatiotemporal distribution of water isotope ratios across a single metropolitan area. This result highlights the potential of stable isotopes as a tool to study and monitor the function of municipal water systems at finer scales than demonstrated in previous regional to national-scale examples. The ability to distinguish and "map" the structure of multisource municipal water systems may be useful in a variety of contexts, including investigation of water rights and contamination cases and validation of physical models for the operation of water systems. Our data suggest that information on water system structure will also be critical to the development of improved models of local-scale water isotopic variation that may increase the robustness of forensic applications of stable isotopes, and we demonstrate one such model for the SLV study area. Last, we show that our data set of SLV tap water isotope ratios reveals changes that can be attributed to the influence of changing climatic conditions on regional water supplies. This provides information relevant to planning for future water security within the rapidly growing SLV metropolitan area, and implies that carefully structured isotopic monitoring may offer unique information in support of diagnosis, planning, and management of water supply resilience in other urban centers subject to future stress from changing climatic conditions.

Acknowledgments
We thank the numerous volunteers who assisted with the SLV tap water surveys. This work was supported by U.S. National Science Foundation grants EF-1137336, 124012, 01241286, and 1208732, and National Institute of Justice grants 2011-DN-BX-K544 and 2013-DN-BX-K009. Data sets analyzed within this study are available in the supporting information.

References

Aggarwal, P. K., K. F. Froehlich, and J. R. Gat (2005), *Isotopes in the Water Cycle*, Springer, Netherlands.
Bardsley, T., A. Wood, M. Hobbins, T. Kirkham, L. Briefer, J. Niermeyer, and S. Burian (2013), Planning for an uncertain future: Climate change sensitivity assessment toward adaptation planning for public water supply, *Earth Interact.*, *17*, 1–26, doi:10.1175/2012EI000501.1.
Bartelink, E. J., G. E. Berg, M. M. Beasley, and L. A. Chesson (2014), Application of stable isotope forensics for predicting region of origin of human remains from past wars and conflicts, *Ann. Anthropol. Pract.*, *38*(1), 124–136.
Baskin, R. L., K. M. Waddell, S. A. Thiros, E. M.Giddings, H. K. Hadley, D. W. Stephens, and S. J.Gerner (2002), Water-Quality Assessment of the Great Salt Lake Basins, Utah, Idaho, and Wyoming: Environmental Setting and Study Design, *U.S. Geol. Surv. Water Resour. Invest. Rep. 02-4115*, 47 pp.
Bates, B. C., Z. W. Kundzewicz, S. Wu, and J. P. Palutikof (2008), *Climate Change and Water, Tech. Pap. VI*, Intergovernmental Panel on Climate Change, IPCC Secretariat, Geneva, 210 pp.
Bexfield, L. M., S. A. Thiros, D. W. Anning, J. M. Huntington, and T. S. McKinney (2011), Effects of natural and human factors on groundwater quality of basin-fill aquifers in the southwestern United States-conceptual models for selected contaminants, *U.S. Geol. Surv. Sci. Invest. Rep.2328-0328*, 90 p.
Bowen, G. J. (2010), Isoscapes: Spatial pattern in isotopic biogeochemistry, *Annu. Rev. Earth Planet. Sci.*, *38*, 161–187.
Bowen, G. J., and B. Wilkinson (2002), Spatial distribution of δ18O in meteoric precipitation, *Geology*, *30*(4), 315–318.
Bowen, G. J., L. I. Wassenaar, and K. A. Hobson (2005a), Global application of stable hydrogen and oxygen isotopes to wildlife forensics, *Oecologia*, *143*(3), 337–348.
Bowen, G. J., D. A. Winter, H. J. Spero, R. A. Zierenberg, M. D. Reeder, T. E. Cerling, and J. R. Ehleringer (2005b), Stable hydrogen and oxygen isotope ratios of bottled waters of the world, *Rapid Commun. Mass Spectrom.*, *19*(23), 3442–3450.
Bowen, G. J., T. E. Cerling, and J. R. Ehleringer (2007a), Stable isotopes and human water resources: Signals of change, *Terr. Ecol.*, *1*, 283–300.
Bowen, G. J., J. R. Ehleringer, L. A. Chesson, E. Stange, and T. E. Cerling (2007b), Stable isotope ratios of tap water in the contiguous United States, *Water Resour. Res.*, *43*, W03419, doi:10.1029/2006WR005186.
Bowen, G. J., C. D. Kennedy, P. D. Henne, and T. Zhang (2012), Footprint of recycled water subsidies downwind of Lake Michigan, *Ecosphere*, *3*(6), 53.
Buckley, J. (2013), Quantifying the impacts of interbasin transfers on water balances in the conterminous United States, MS thesis, N. C.State Univ., Raleigh.
Chen, X.-L., H.-M. Zhao, P.-X. Li, and Z.-Y. Yin (2006), Remote sensing image-based analysis of the relationship between urban heat island and land use/cover changes, *Remote Sens. Environ.*, *104*(2), 133–146.
Chesson, L. A., L. O. Valenzuela, S. P. O'Grady, T. E. Cerling, and J. R. Ehleringer (2010), Links between purchase location and stable isotope ratios of bottled water, soda, and beer in the United States, *J. Agric. Food Chem.*, *58*(12), 7311–7316.
Clark, I., and P. Fritz (1997), *Environmental Isotopes in Hydrogeology*, pp.328, CRC press, Boca Raton, Fla.
Craig, H. (1961), Isotopic variations in meteoric waters, *Science*, *133*(3465), 1702–1703.
Craig, H., and L. I. Gordon (1965), Deuterium and oxygen-18 variations in the ocean and marine atmosphere, in *Stable Isotopes in Oceanographic Studies and Paleo-Temperatures*, edited by E. Tongiorgi, pp. 9–130, Lab. Geol. Nuc., Pisa.
Craig, R. (2010), 'Stationarity is dead'-long live transformation: Five principles for climate change adaptation law, *Harv. Envtl. L. Rev.*, *34*(1), 9–75.
Dansgaard, W. (1964), Stable isotopes in precipitation, *Tellus*, *16*, 436–468.
Darling, W. (2004), Hydrological factors in the interpretation of stable isotopic proxy data present and past: A European perspective, *Quat. Sci. Rev.*, *23*(7), 743–770.
Darling, W., A. Bath, and J. Talbot (2003), The O and H stable isotope composition of freshwaters in the British Isles. 2, surface waters and groundwater, *Hydrol. Earth Syst. Sci.*, *7*, 183–195.
Dawson, T. E., and R. Siegwolf (2011), *Stable Isotopes as Indicators of Ecological Change*, Academic Press, San Diego.
Dutton, A., B. H. Wilkinson, J. M. Welker, G. J. Bowen, and K. C. Lohmann (2005), Spatial distribution and seasonal variation in 18O/16O of modern precipitation and river water across the conterminous USA, *Hydrol. Processes*, *19*(20), 4121–4146.
Ehleringer, J. R., G. J. Bowen, L. A. Chesson, A. G. West, D. W. Podlesak, and T. E. Cerling (2008), Hydrogen and oxygen isotope ratios in human hair are related to geography, *Proc. Natl. Acad. Sci. U. S. A.*, *105*(8), 2788–2793.
Ehleringer, J. R., J. E. Barnette, Y. Jameel, B. J. Tipple, and G. J. Bowen (2016), Urban water: A new frontier in isotope hydrology, *Isot. Environ. Health Stud.*, 1–10, doi:10.1080/10256016.2016.1171217.

Evaristo, J., S. Jasechko, and J. J. McDonnell (2015), Global separation of plant transpiration from groundwater and streamflow, *Nature*, *525*(7567), 91–94.
Fort, D., B. Nelson, K. Coplin, and S. Wirth (2012), *Pipe Dreams: Water Supply and Pipeline Projects in the West*, Natl. Resour. Def. Counc., Washington, D. C.
Fry, B. (2007), *Stable Isotope Ecology*, Springer, N. Y.
Gat, J. (1995), Stable isotopes of fresh and saline lakes, in *Physics and Chemistry of Lakes*, pp. 139–165, Springer Verlag, Berlin Heidelberg.
Gat, J. (1996), Oxygen and hydrogen isotopes in the hydrologic cycle, *Annu. Rev. Earth Planet. Sci.*, *24*(1), 225–262.
Geldern, R., and J. A. Barth (2012), Optimization of instrument setup and post-run corrections for oxygen and hydrogen stable isotope measurements of water by isotope ratio infrared spectroscopy (IRIS), *Limnol. Oceanogr. Methods*, *10*(12), 1024–1036.
Gibson, J., and R. Reid (2014), Water balance along a chain of tundra lakes: A 20-year isotopic perspective, *J. Hydrol.*, *519*, 2148–2164.
Gibson, J., S. Birks, and T. Edwards (2008), Global prediction of δA and δ2H-δ18O evaporation slopes for lakes and soil water accounting for seasonality, *Global Biogeochem. Cycles*, *22*, *GB2031*, doi:10.1029/2007GB002997.
Gibson, J. J., S. J. Birks, and Y. Yi (2016), Stable isotope mass balance of lakes: A contemporary perspective, *Quat. Sci. Rev.*, *131*, 316–328.
Good, S. P., C. D. Kennedy, J. C. Stalker, L. A. Chesson, L. O. Valenzuela, M. M. Beasley, J. R. Ehleringer, and G. Bowen (2014a), Patterns of local and nonlocal water resource use across the western US determined via stable isotope intercomparisons, *Water Resour. Res.*, *50*, 8034–8049, doi:10.1002/2014WR015884.
Good, S. P., D. V. Mallia, J. C. Lin, and G. J. Bowen (2014b), Stable isotope analysis of precipitation samples obtained via crowdsourcing reveals the spatiotemporal evolution of Superstorm Sandy, *PloS one*, *9*(3), e91117.
Good, S. P., D. Noone, and G. Bowen (2015), Hydrologic connectivity constrains partitioning of global terrestrial water fluxes, *Science*, *349*(6244), 175–177.
Grootes, P., M. Stuiver, J. White, S. Johnsen, and J. Jouzel (1993), Comparison of oxygen isotope records from the GISP2 and GRIP Greenland ice core, *Nature*, *366*(6455), 552–554.
Gupta, R., and P. R. Bhave (1994), Reliability analysis of water-distribution systems, *J. Environ. Eng.*, *120*(2), 447–461.
Hobson, K. A., and L. I. Wassenaar (1996), Linking breeding and wintering grounds of neotropical migrant songbirds using stable hydrogen isotopic analysis of feathers, *Oecologia*, *109*(1), 142–148.
Hobson, K. A., L. Atwell, and L. I. Wassenaar (1999), Influence of drinking water and diet on the stable-hydrogen isotope ratios of animal tissues, *Proc. Natl. Acad. Sci. U. S. A.*, *96*(14), 8003–8006.
Jardine, A., R. Merideth, M. Black, and S. LeRoy (2013), *Assessment of Climate Change in the Southwest United States: A Report Prepared for the National Climate Assessment*, Island Press, Washington, D. C.
Kendall, C., and T. B. Coplen (2001), Distribution of oxygen-18 and deuterium in river waters across the United States, *Hydrol. Processes*, *15*(7), 1363–1393.
Kennedy, C. D., G. J. Bowen, and J. R. Ehleringer (2011), Temporal variation of oxygen isotope ratios (δ 18 O) in drinking water: Implications for specifying location of origin with human scalp hair, *For. Sci. Int.*, *208*(1), 156–166.
Kuttler, W., S. Weber, J. Schonnefeld, and A. Hesselschwerdt (2007), Urban/rural atmospheric water vapour pressure differences and urban moisture excess in Krefeld, Germany, *Int. J. Climatol.*, *27*(14), 2005–2015.
Landwehr, J. M., T. B. Coplen, and D. W. Stewart (2014), Spatial, seasonal, and source variability in the stable oxygen and hydrogen isotopic composition of tap waters throughout the USA, *Hydrol. Processes*, *28*(21), 5382–5422.
Leslie, D., K. Welch, and W. Lyons (2014), Domestic water supply dynamics using stable isotopes δ18O, δD, and d-Excess, *J. Water Resour. Protection*, *6*, 1517–1532.
Liggett, J. A., and L.-C. Chen (1994), Inverse transient analysis in pipe networks, *J. Hydraul. Eng.*, *120*(8), 934–955.
Nielson, K. E., and G. J. Bowen (2010), Hydrogen and oxygen in brine shrimp chitin reflect environmental water and dietary isotopic composition, *Geochim. Cosmochim. Acta*, *74*(6), 1812–1822.
O'Brien, D. M., and M. J. Wooller (2007), Tracking human travel using stable oxygen and hydrogen isotope analyses of hair and urine, *Rapid Commun. Mass Spectrom.*, *21*(15), 2422–2430.
R Core Team (2015), *R: A Language and Environment for Statistical Computing, R Found. for Stat. Comput.*, Vienna, Austria.
Rodell, M., I. Velicogna, and J. S. Famiglietti (2009), Satellite-based estimates of groundwater depletion in India, *Nature*, *460*(7258), 999–1002.
Schoeller, D. A., M. Minagawa, R. Slater, and I. Kaplan (1986), Stable isotopes of carbon, nitrogen and hydrogen in the contemporary North American human food web, *Ecol. Food Nutr.*, *18*(3), 159–170.
Seckler, D., R. Barker, and U. Amarasinghe (1999), Water scarcity in the twenty-first century, *Int. J. Water Resour. D.*, *15*(1-2), 29–42.
Skrzypek, G., A. Mydłowski, S. Dogramaci, P. Hedley, J. J. Gibson, and P. F. Grierson (2015), Estimation of evaporative loss based on the stable isotope composition of water using Hydrocalculator, *J. Hydrol.*, *523*, 781–789.
Smith, G. I., I. Friedman, G. Veronda, and C. A. Johnson (2002), Stable isotope compositions of waters in the Great Basin, United States 3. Comparison of groundwaters with modern precipitation, *J. Geophys. Res.*, *107*(D19), 4402, doi:10.1029/2001JD000567.
Thiros, S. A. (2003), Quality and sources of shallow ground water in areas of recent residential development in Salt Lake Valley, Salt Lake County, Utah, *U.S. Geol. Surv. Water Resour. Invest. Rep. 03*-4028, 107 pp.
Thiros, S. A., and A. H. Manning (2004), Quality and sources of ground water used for public supply in Salt Lake Valley, Salt Lake County, Utah, 2001, *U.S. Geol. Surv. Water Resour. Invest. Rep. 03-4325*, 95 pp.
Vogt, H. (1976), Isotopentrennung bei der Verdunstung von Wasser, Staatsexamensarbeit, Inst. für Umweltphysik, Heidelberg, Germany.
Waldrip, S. H., R. K. Niven, M. Abel, and M. Schlegel (2016), Maximum Entropy Analysis of Hydraulic Pipe Flow Networks, *J. Hydraul. Eng.*, 04016028, doi:10.1061/(ASCE)HY.1943-7900.0001126.
Wassenaar, L., S. Van Wilgenburg, K. Larson, and K. Hobson (2009), A groundwater isoscape (δD, δ 18 O) for Mexico, *J. Geochem. Explor.*, *102*(3), 123–136.
West, J. B., G. J. Bowen, T. E. Dawson, and K. P. Tu (2010), *Isoscapes*, Springer, N. Y.
Williams, A. E. (1997), Stable isotope tracers: Natural and anthropogenic recharge, Orange County, California, *J. Hydrol.*, *201*(1), 230–248.